Chemical Vapor Deposition

Full Paper

Light-Induced CVD of Titanium Dioxide Thin Films II: Thin Film Crystallinity**

By *Estelle Halary-Wagner*, *Frank R. Wagner*, *Arnaud Brioude*, *Jacques Mugnier*, and *Patrik Hoffmann**

Titanium dioxide thin films are obtained by CVD on low temperature (60–210 °C) substrates using perpendicular irradiation from a long pulse XeCl excimer laser (308 nm). The precursor, *tetra*-isopropoxide titanium, is used in an oxygen-containing atmosphere with a total pressure of 10 mbar in the chamber. X-ray photoelectron spectroscopy (XPS) analyses show that the chemical composition of the film, independent of the deposition parameters, is TiO_2 with some additional surface carbon contamination. Depending on deposition parameters, the film crystallinity varies between amorphous, anatase, and rutile. Numerical temperature simulations and sample characterization show that the crystalline state of the deposited material evolves from amorphous to anatase to rutile with an increase in the laser-induced temperature. Additionally, substrate temperature and laser repetition rate strongly influence the phase-transition behavior.

Keywords: Anatase, Excimer laser, Rutile, Titanium dioxide

1. Introduction

Light-induced (LI) CVD uses photon irradiation to promote or activate a CVD reaction. The use of excimer lasers (powerful UV pulsed-light sources) perpendicularly irradiating the substrate was shown to be a promising technique for growing a large number of oxides at low substrate temperature (see references in E. Halary-Wagner et al.[1]). The UV photons can activate the deposition reaction in various ways:[2,3]

- Photolytically, when light absorption by the precursor induces an electronic transition excitation leading to the precursor dissociation by internal energy relaxation.
- Pyrolytically, when light absorption in the substrate (or in the film) activates a thermal decomposition of the precursor.
- Photocatalytically, when light absorption in the substrate (or in the film) induces electronic transitions generating electrons and holes responsible for redox reactions of adsorbed precursor molecules on the surface.

We focus here on TiO_2 deposition from titanium *tetra*-isopropoxide (TTIP) in an oxygen-containing atmosphere induced by irradiation using a long pulse (250 ns) XeCl excimer laser (308 nm). In this system, the deposition was shown to be induced photolytically with an Arrhenius dependence on the substrate temperature.[1] In addition to the activation of the chemical reaction leading to the deposition, the excimer laser photons interact photochemically or thermally with the substrate or the already deposited oxide film. Other processes, such as TiO_2 crystallization under irradiation (sol–gel,[4,5] or amorphous gas phase deposited films[6]) or oxide ablation (for instance, ITO electrode structuration[7]), benefit from these interactions.

Although LICVD is usually considered as a low temperature technique, due to the low substrate temperature, excimer laser irradiation of oxide films (which normally absorb light at excimer wavelengths) induces a temperature rise during very short time periods, as shown by laser-induced temperature rise simulations.[8] In the present work, a numerical approach was used to estimate the laser-induced temperature rise of the film in the experimental deposition conditions used, and laser-induced temperatures up to 1400 °C were found.

Titanium dioxide, which has been studied in this work, is a widely used material. Using CVD methods, amorphous material is usually deposited at low substrate temperature, while crystalline phases, mainly anatase and rutile, are successively obtained with increasing substrate temperature.[9] Depending on the target application, one crystalline form may be preferable for instance, amorphous films are required for optical coatings,[10] while anatase layers are preferred for photochemically active layers,[11] and rutile ones are investigated for micro-electronic coatings,[12] so it is advantageous to be able to selectively deposit each phase.

[*] Dr. P. Hoffmann, Dr. E. Halary-Wagner, Dr. F. R. Wagner, Dr. A. Brioude
Advanced Photonics Laboratory
Ecole Polytechnique Fédérale de Lausanne (EPFL)
CH-1015 Lausanne-EPFL (Switzerland)
E-mail: patrik.hoffmann@epfl.ch
Prof. J. Mugnier
Laboratoire de Physico-chimie des Matériaux Luminescents
Université Claude Bernard, Lyon 1
Domaine Scientifique de la Dona
10 rue A.M. Ampère, F-69622 Villeurbanne Cedex (France)

[**] We thank N. Xanthopulos (LMC/DMX/EPFL) for XPS measurements and T. Lippert (PSI, Villigen) for access to Raman microscopy. The authors also gratefully acknowledge James A. DeRose for proof reading the manuscript. This research was supported by grants from the Swiss National Science Foundation (project No. 20-59404.99).

Using our LICVD set-up, the variation from rutile to anatase in the crystalline state of the deposited film, induced by increasing the substrate temperature while irradiating at a low fluence of 150 mJ cm^{-2}, had already been demonstrated in 2000.[13] More recently, Watanabe et al.[14] showed that the crystalline phase of TiO_2 films deposited by LICVD was dependent on substrate temperature, laser repetition rate, and TTIP input, indicating the possible selectivity between anatase and rutile. Under conditions similar to our set-up, films were deposited from TTIP and oxygen, but using a short pulse (20 ns) KrF laser (248 nm). Several other techniques (for instance, liquid phase deposition[15]) also enable the selective deposition, at low temperature, of one TiO_2 crystalline state by varying the process parameters. LICVD however provides the additional advantages of selective area deposition,[16] and precise control of the deposited thickness.[1]

The TiO_2 crystallization processes are inherently complex and not yet completely understood. In particular, the crystallization may depend on many parameters, such as precursor type, deposition chemistry, substrate type, kinetics, etc., influencing the nucleation process. In this work, we will show that the crystalline state of the material deposited by LICVD is mainly dependent upon two things; i) the laser-induced temperature rise, which depends on laser fluence, film thickness, and substrate nature which induces an annealing-like modification of the crystalline state, and ii) a nucleation process which depends on substrate temperature and laser repetition rate.

2. Results

2.1. Chemical Composition

150 nm thick films were deposited on glass at various substrate temperatures (60 °C, 135 °C, and 210 °C) and various laser fluences (100 mJ cm^{-2}, 200 mJ cm^{-2}, and 400 mJ cm^{-2}). These nine films were analyzed by XPS. Measurements were carried out on both as-deposited samples, and those subjected to 1 min sputtering to remove the surface contamination layer. There was no evidence of any influence, either of the substrate temperature or the laser fluence, on the chemical composition of the deposit. Typical spectra are presented in Figure 1 for both the as-deposited samples and those receiving the sputtering treatment.

On the as-deposited samples, the Ti_{2p} region (Fig. 1a) exhibits a doublet at the expected energies for TiO_2 (458.2 ± 0.3 eV for $Ti_{2p_{3/2}}$ and 464 ± 0.3 eV for $Ti_{2p_{1/2}}$).[17] After sputtering, these peaks are highly broadened, exhibiting large shoulders between 452 eV and 458 eV which are typical of the TiO_2 reduction effect under ion bombardment.[17]

On the as-deposited samples, the O_{1s} region (Fig. 1b) exhibits a peak at 529.7 ± 0.8 eV which is the correct position for TiO_2.[17] An important shoulder at higher binding energies, which is usually attributed to adsorbed contamination such as OH, H_2O, O_2, or CO groups[17,18] is also observed. After sputtering, this shoulder is greatly reduced.

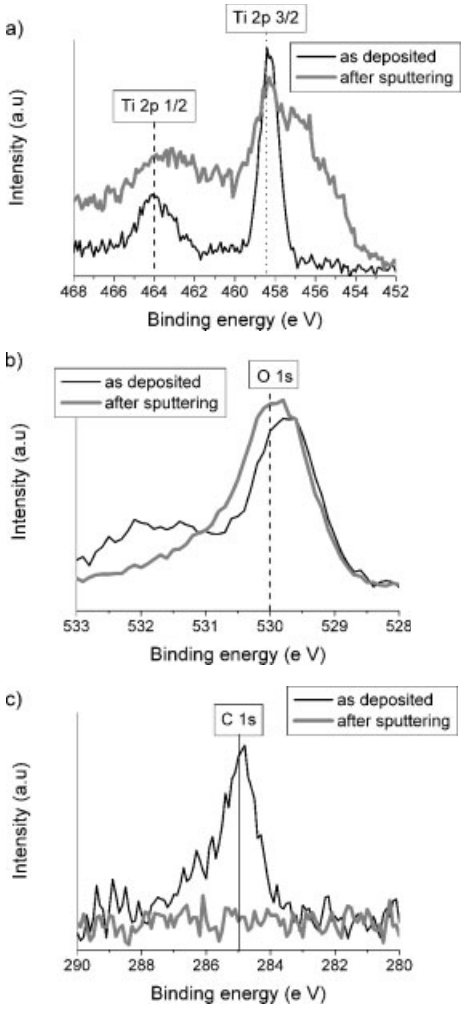

Fig. 1. XPS measurements of a selected sample deposited on glass (150 nm thick TiO_2 film); on the as-deposited sample (black); and after ion sputtering (gray). a) Ti_{2p}, b) O_{1s}, and c) C_{1s} spectra.

The C_{1s} region (Fig. 1c) exhibits a broad peak at 285 eV which disappears in the measurement noise after sputtering.

Chemical composition of the films is evaluated by integrating the XPS peak areas. For the as-deposited samples, the Ti, O, and C atomic concentrations are, respectively, 12.6 ± 2.8 %, 47.8 ± 6.9 %, and 39.6 ± 7.6 %. After 1 min of sputtering, the chemical composition becomes 34.4 ± 3.2 % and 65.4 ± 3.2 % for Ti and O, respectively.

2.2. Crystallinity

Deposits were produced under a large number of experimental conditions and, for each, the crystallinity was evaluated. In parallel, laser-induced temperature rise simulations were carried out under the same experimental conditions.

2.2.1. Effect of Laser Fluence at Different Substrate Temperatures

Two similar sets of experiments were carried out systematically varying the substrate temperature (60 °C, 135 °C, and 210 °C) and the fluence (70–300 mJ cm^{-2}) using a laser repetition rate of 5 Hz.

i) Thirteen films of 1.5 μm thickness were deposited on glass substrates, applying the corresponding required number of pulses between 1.3×10^4 and 4.1×10^5 for each condition (see Fig. 4c below). The crystallinity of these deposits was analyzed by Raman spectroscopy and the spectra are presented in Figure 2. Details of Raman analysis of TiO_2 are given in the Experimental section.

ii) Nine films of 150 nm thickness were deposited on silicon substrates, applying the corresponding required number of pulses between 1.3×10^3 and 4.1×10^4 for each condition (see Fig. 4f below). The crystallinity of these deposits was analyzed by transmission electron microscopy (TEM) and electron diffraction (Fig. 3).

The laser-induced temperature rise by a single pulse was estimated for both sets of experiments and results are presented in Figure 4. Figures 4a and 4d show typical temporal temperature profiles compared to the temporal laser pulse profile, while Figures 4b and 4e show typical depth profiles. The maximum surface temperatures obtained are reported in Figures 4c and 4f, as are the number of pulses.

In the Case of Thick Films on Glass: Depending on the laser fluence and substrate temperature, anatase, rutile, or anatase/rutile mixtures are detected (summarized in Fig. 2d). At a given substrate temperature and with increasing laser fluence, anatase gives way to rutile. This transition from anatase to rutile takes place at a higher fluence when the substrate temperature increases. Additionally, in some of the spectra, parasitic peaks appear together as a broad band around 350 cm^{-1} and there is a peak at 510 cm^{-1}, all of which are characteristic of suboxides,[19] believed to be present at the film-glass interface.

The laser-induced temperature rise simulations show that laser pulses induce large temperature gradients (several hundreds of degrees Celsius over 1.5 μm) in the film, which remains heated for more than 1 ms. The maximum temperature increases almost linearly with the fluence from 350 °C at 100 mJ cm^{-2} to 1670 °C on the surface at 400 mJ cm^{-2} (see Fig. 4c).

In the Case of Thin Films on Si: Depending on laser fluence and substrate temperature, amorphous phase, anatase, anatase/rutile mixtures, or rutile are detected (summarized in Fig. 3b). At 60 °C, increasing the fluence leads to the appearance of anatase crystals in the amorphous matrix, while at 135 °C and 210 °C, the amount of rutile in the anatase/rutile mixture increases.

The laser-induced temperature rise simulations show that laser pulses generate temperature gradients (about 100 °C over 150 nm) in the film, which remains heated for about 10 μs. The maximum surface temperature increases almost linearly with fluence from 162 °C at 100 mJ cm^{-2} to 635 °C on the film surface at 300 mJ cm^{-2} (see Fig. 4f).

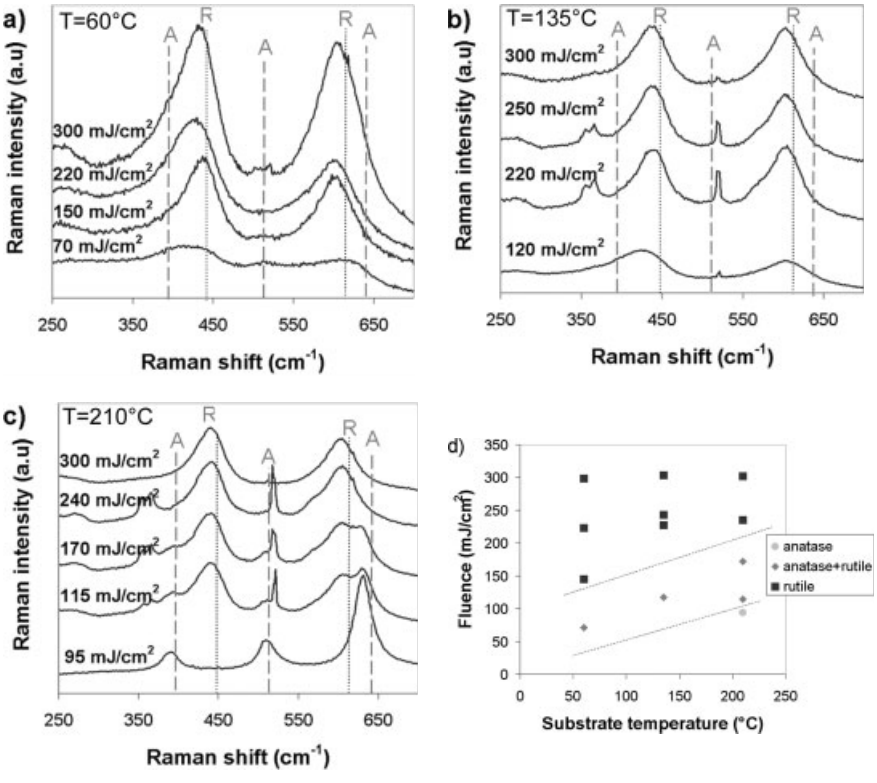

Fig. 2. Raman spectra of 1.5 μm thick TiO_2 films deposited on glass at various substrate temperatures and laser fluences. a) 60 °C, b) 135 °C, and c) 210 °C. The theoretical peak positions for anatase (A) and rutile (R) are indicated. The shift of the experimental peaks with respect to the theoretical positions is believed to be due to a calibration error of the spectrometer. d) Summary of the TiO_2 crystalline phase measured by Raman spectroscopy under the various conditions.

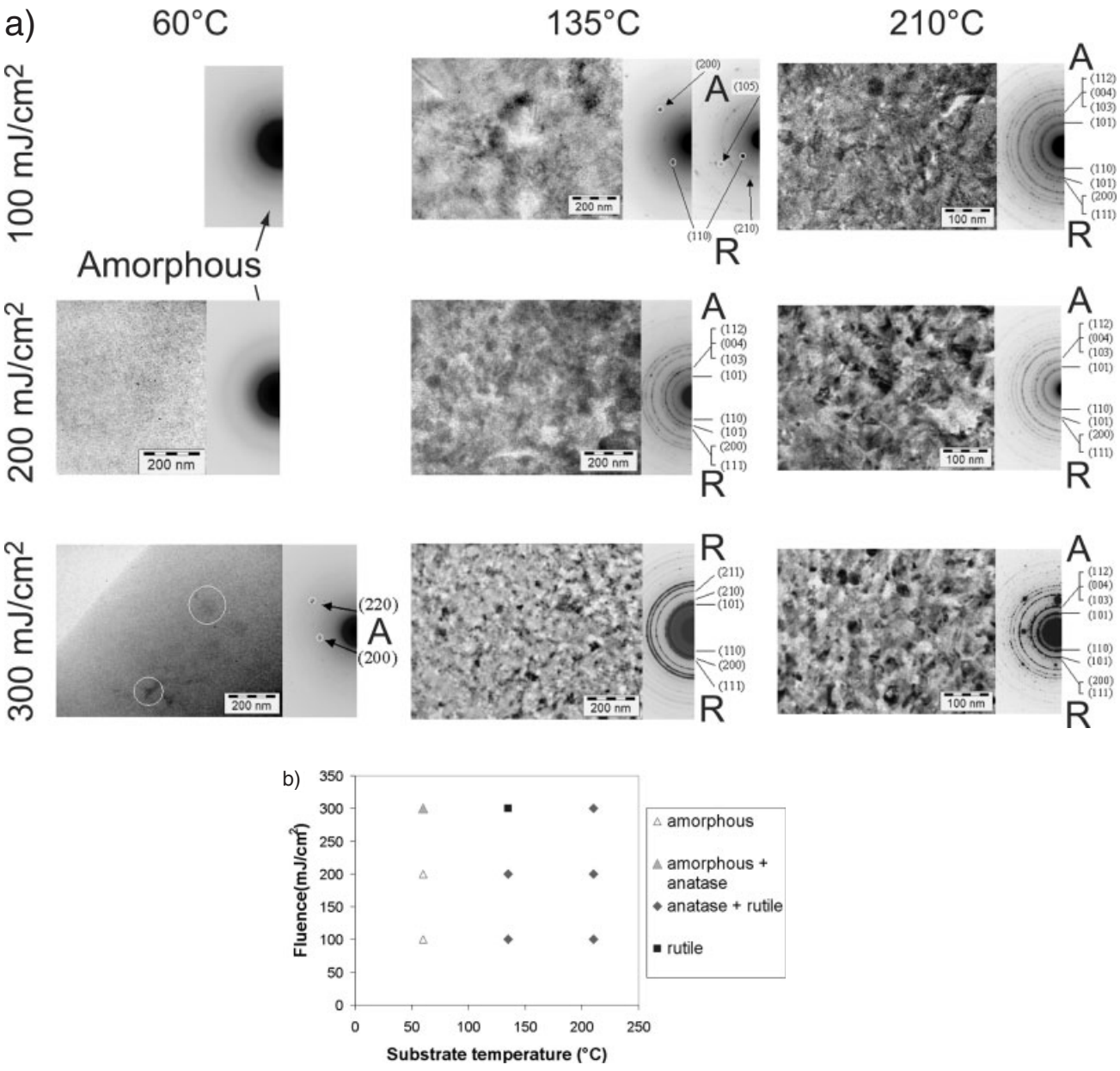

Fig. 3. a) TEM bright-field images and associated diffractograms of 150 nm thin TiO_2 films deposited on silicon substrate with various conditions of substrate temperature and laser fluence (A, anatase; R, rutile). b) Summary of the crystalline phases encountered under the various conditions.

2.2.2. Influence of the Deposited Thickness

Multi-step deposits were made on silicon substrates at $T = 210\,^{\circ}C$, $F = 400$ mJ cm^{-2}, and $f = 5$ Hz, with the deposited thickness varying from 150 nm to 2.7 μm (see Fig. 5a). The micro-Raman spectra recorded on the various steps are presented in Figure 5b.

The Raman spectra show that the film is pure rutile at the highest thicknesses, while for the lowest thicknesses, some anatase is also present.

The laser-induced temperature rise by a single pulse was estimated for different thickness of TiO_2 films deposited on silicon under the same experimental conditions ($T = 210\,^{\circ}C$, $F = 400$ mJ cm^{-2}, see Fig. 6a). The maximum film surface temperature increases with a film thickness increase, saturating at a film thickness of around 800 nm where it reaches the bulk TiO_2 temperature rise value of 1680 °C. The film/substrate interface is less and less heated as a larger thickness of TiO_2 is considered.

2.2.3. Influence of the Laser Repetition Rate

Several 300 nm thick TiO_2 films were deposited on glass at 210 °C and at two different fluences while varying the laser repetition rate (1 Hz, 5 Hz, 10 Hz, and 20 Hz). Raman spectra of these films are presented in Figure 7.

Chemical Vapor Deposition

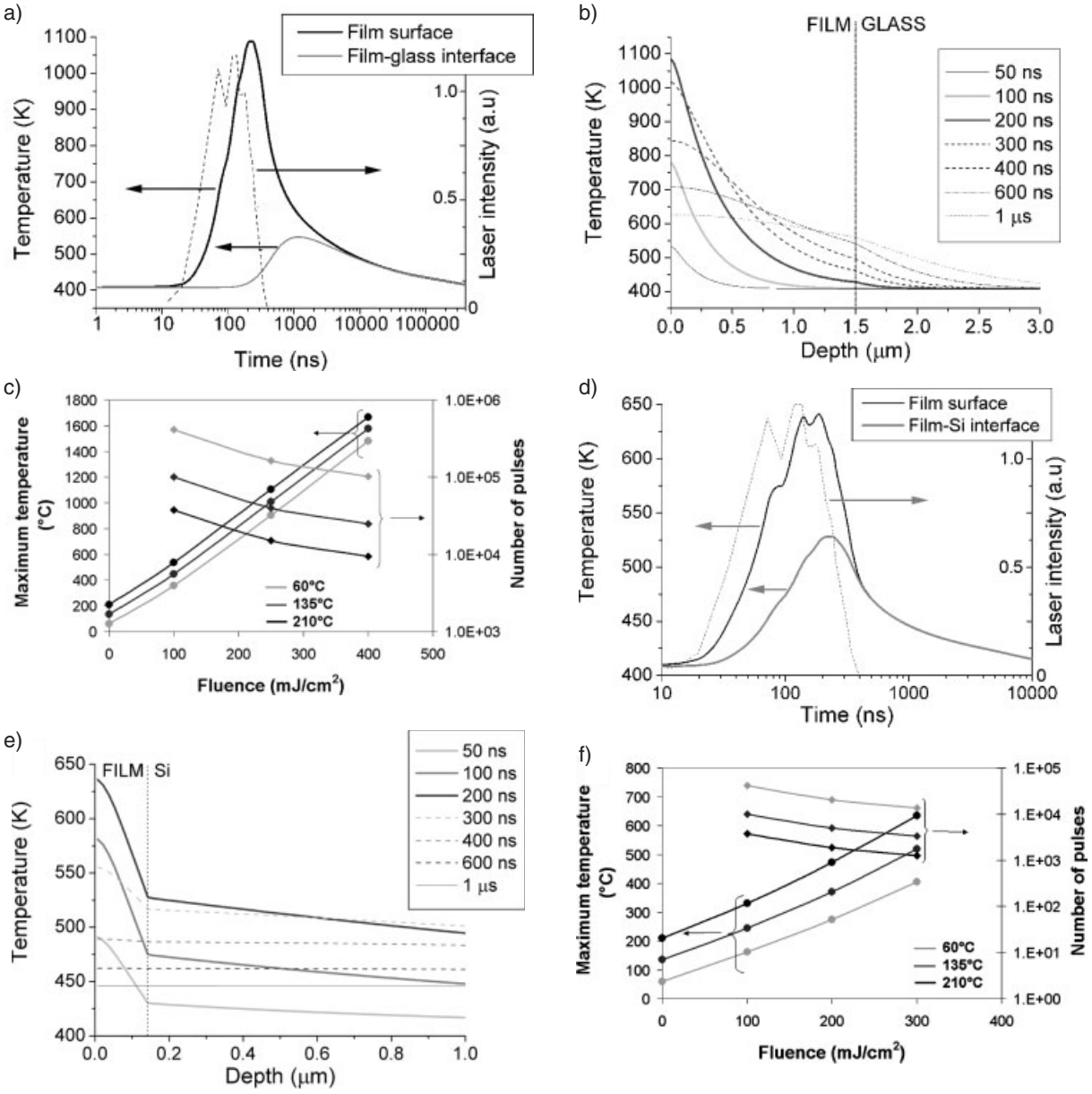

Fig. 4. Laser-induced temperature evolution for 1.5 μm thick TiO_2 films on glass (a–c) and for 150 nm thick TiO_2 films on silicon (d–f). a) and d) Typical temporal profiles for $T = 135\,^{\circ}C$ and $F = 200\ mJ\ cm^{-2}$, to be compared with the laser pulse temporal profile. b,e) Typical depth profiles for $T = 135$ C and $F = 200\ mJ\ cm^{-2}$. c,f) Number of pulses required to deposit the TiO_2 films and maximum laser-induced surface temperature rise.

At the lower fluence (55 mJ cm^{-2}), the crystalline state of the deposited film varies from amorphous at 1 Hz to anatase at higher repetition rates (see Fig. 7a). At the higher fluence (210 mJ m^{-2}), the crystalline state changes from a mixture of anatase and rutile to mainly rutile at higher repetition rates (see Fig. 7b).

Laser-induced temperature rise and cooling after the pulse were simulated for a single pulse corresponding to the experimental conditions applied (300 nm TiO_2 film on glass, $T = 210\,^{\circ}C$, $F = 55\ mJ\ cm^{-2}$, and $F = 210\ mJ\ cm^{-2}$) and under similar conditions at a higher fluence ($F = 400\ mJ\ cm^{-2}$) (see Fig. 8a). For comparison, similar simulations were carried out on silicon substrates (see Fig. 8b). The simulations show that the film and substrate are cooled after 1 ms on glass and 0.1 ms on silicon.

3. Discussion

3.1. Chemical Composition

The results of films analysis by XPS suggest that the deposited material is close to stoichiometric TiO_2. No sub-oxide shoulders are detected in the Ti_{2p} spectrum on the as-deposited sample and, after ion sputtering, the measured value for $O/Ti = 1.9 \pm 0.3$. No carbon contamination is

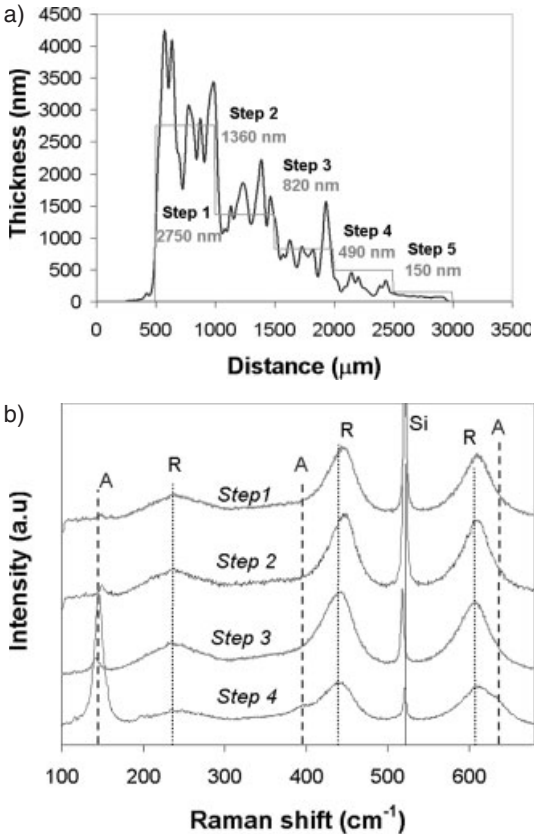

Fig. 5. Influence of the film thickness on the crystallinity. a) Profile of a step deposit on silicon ($T = 210\,^{\circ}C$, $F = 400$ mJ cm^{-2}, $f = 5$ Hz, $N = 1500$–15000 pulses). b) Micro-Raman spectra measured on the different steps. The theoretical peak positions for anatase (A) and rutile (R) are indicated, together with the Raman scattering peak for the silicon substrate (Si).

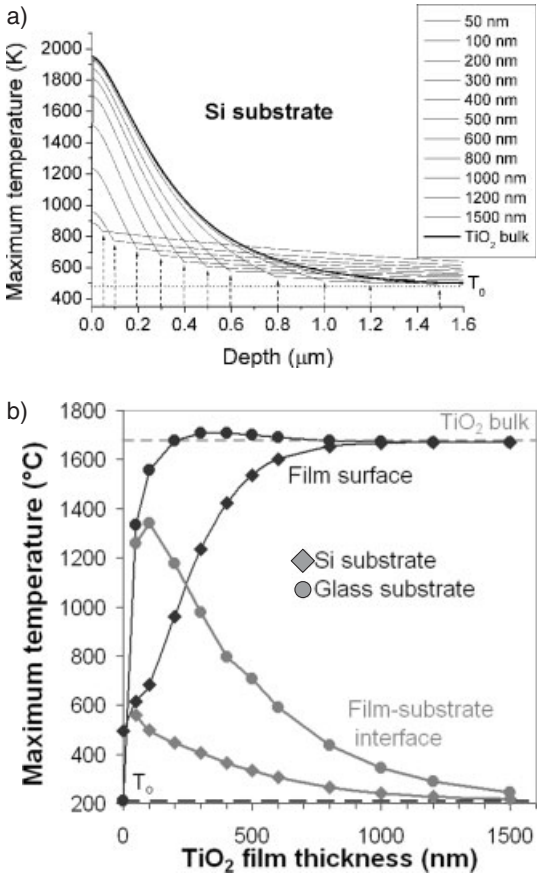

Fig. 6. Laser-induced temperature rise for various TiO_2 film thicknesses ($T = 210\,^{\circ}C$, $F = 400$ mJ cm^{-2}). a) Calculated temperature depth profiles on a Si substrate (the arrows indicate the interface between the film and the substrate for the various TiO_2 film thicknesses) and b) Maximum film surface temperature on Si (◆) and glass (●) substrates, and film-interface temperature for the maximum surface temperature as a function of TiO_2 film thickness on Si (◇) and on glass (○).

observed in the bulk, but a standard surface layer of contamination is detected on as-deposited samples.

3.2. Crystallinity

Raman and TEM analyses carried out on films deposited under different experimental conditions show that the crystalline state depends on several process parameters; i.e., substrate temperature, laser fluence, substrate nature, film thickness, and laser repetition rate. Depending on the experiment, an amorphous state, or the presence of anatase and/or rutile phases are detected.

Upon comparison with the laser-induced temperature rise simulations carried out for each of the experimental conditions, two effects are found to be superimposed.

i) With increasing laser-induced temperature rise, the crystalline state changes from amorphous to anatase to rutile, i.e., from the low temperature to the high temperature phases (details in Section 3.2.1), therefore this seems to be an annealing-like process.

ii) With increasing substrate temperature or with decreasing laser pulse repetition rate, a phase change from amorphous to anatase to rutile takes place for higher laser-induced temperature rises (details in Section 3.2.2).

3.2.1. Laser-Induced Temperature Rise Effect: Phase Transition from Amorphous to Anatase to Rutile, Annealing-Like Mechanism

Let us label ΔT_{laser} the simulated laser-induced temperature rise (at constant substrate temperature and at constant laser repetition rate). The crystallinity analyses for the different experimental conditions tested show that the increase of ΔT_{laser} correlates with a phase transition from amorphous to anatase to rutile, i.e., from low temperature phases to high temperature phases. The laser-induced temperature rise is influenced by various parameters:

i) *Laser Fluence*: ΔT_{laser} increases almost linearly with laser fluence (see Fig. 4c and Fig. 4f). For any given condition, increasing the laser fluence always induces a change to a higher crystalline state; either from amorphous to anatase (e.g., at 60 °C, 150 nm TiO_2 on Si, see Fig. 3), or

Chemical Vapor Deposition

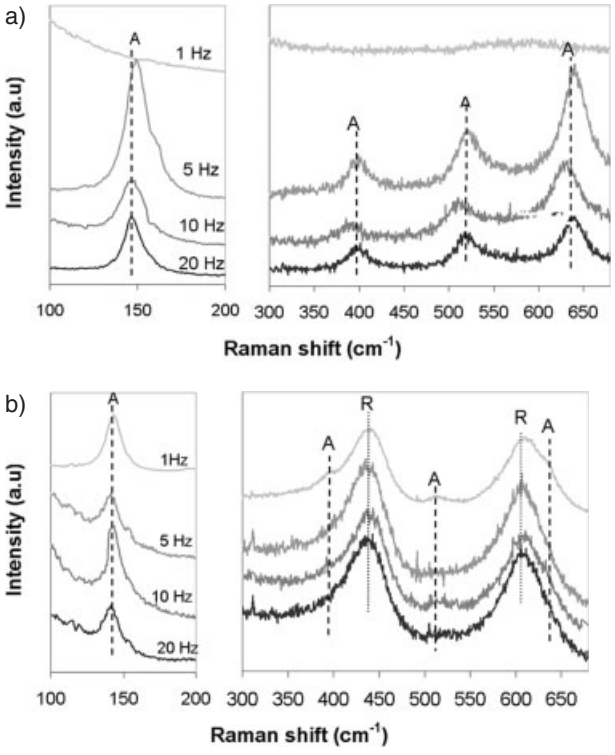

Fig. 7. Raman spectra of a 300 nm thick TiO_2 film deposited on glass at 210 °C and different repetition rates for two different fluences: a) $F = 55$ mJ cm^{-2} and b) $F = 210$ mJ cm^{-2}. The anatase peak at 143 cm^{-1} is presented on a separate scale from the rest of the spectrum as it is approximately five to ten times more intense. The theoretical peak positions for anatase (A) and rutile (R) are indicated.

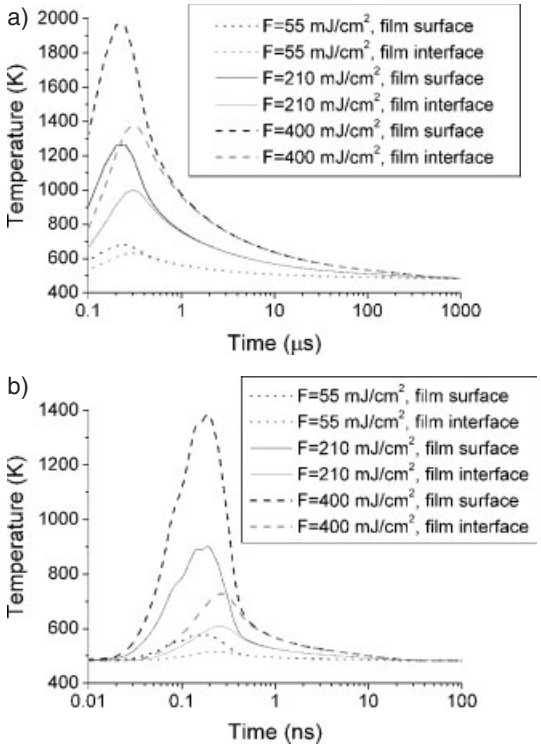

Fig. 8. Laser-induced heating and cooling for a single pulse onto a 300 nm thick TiO_2 film at $T = 210$ °C for three different fluences (55 mJ cm^{-2}, 210 mJ cm^{-2}, and 400 mJ cm^{-2}): a) on a glass substrate; and b) on a silicon substrate.

from anatase to rutile (e.g., at 210 °C, 1.5 μm TiO_2 on glass, see Fig. 2).

ii) *TiO_2 Film Thickness*: simulations show that ΔT_{laser} increases significantly with the film thickness (see Fig. 6). Experimentally, a transformation from a mixture of anatase and rutile to pure rutile (i.e., from a lower temperature phase to a higher temperature phase) is found when increasing the film thickness on a Si substrate from 150 nm to 820 nm (see Fig. 5). In more detail, ΔT_{laser} increases with film thickness until the saturation temperature which corresponds to the laser-induced temperature rise in bulk TiO_2. The bulk temperature rise is obtained for a TiO_2 thickness corresponding roughly to the heat penetration depth, l_T, in the film ($l_T = 2\sqrt{D\tau} = 870$ nm, with D being the film diffusivity and τ the pulse duration). As a matter of fact, as soon as the film thickness exceeds the optical penetration depth, l_λ ($l_\lambda = \alpha^{-1} = 40$ nm, where α is the absorption coefficient), the light is mainly absorbed in the film from which the generated heat must diffuse away. The shape of the curve depends on the difference in heat diffusivities between the film and substrate (see Fig. 6b):

- if the film thermal diffusivity is lower than the substrate diffusivity (which is the case for TiO_2 on Si), the thinner the film, the more efficiently it is cooled. Therefore, ΔT_{laser} increases with the film thickness until it saturates for l_T.
- if the film thermal diffusivity is higher than the substrate diffusivity (which is the case for TiO_2 on glass), the heat tends to remain longer in the film and consequently, a higher ΔT_{laser} rise than for bulk TiO_2 is obtained before saturation is reached.

iii) *Substrate Nature*: Figure 8 shows that under similar conditions, much higher ΔT_{laser} values are obtained on glass than on silicon substrates, and that films on glass are heated for a longer time. This can again be explained by the higher heat diffusivity of silicon compared to glass leading to a faster heat dissipation during the pulse resulting in a lower ΔT_{laser} in the film. Experimentally, lower temperature crystalline structures are obtained on Si than on glass, again associated with a lower ΔT_{laser}. For instance, a pure rutile phase is obtained for a 300 nm thick film on glass at $T = 210$ °C, $F = 210$ mJ cm^{-2} and $f = 5$ Hz (Fig. 7b) while, although at a higher fluence, some anatase is still detected in approximately the same film thickness on Si, $T = 210$ °C, $F = 400$ mJ cm^{-2}, and $f = 5$ Hz (Fig. 5b).

In conclusion, the observed film crystallinity depends upon the fluence, film thickness, and substrate, and can be explained by an in-situ laser-annealing mechanism during the pulse.

3.2.2. Substrate Temperature and Laser Repetition Rate Effect: Influence on the Position of the Phase Transition and Reaction Pathway Effects

The transition fluences from amorphous to anatase and from anatase to rutile are highly dependent on the *substrate temperature* (Fig. 2d and Fig. 3b). The transition from amorphous to anatase tends to take place at higher fluences for lower substrate temperature while the transition from anatase to rutile takes place at higher fluences with increasing substrate temperature. At low fluence, the observation of rutile at lower substrate temperatures than those for anatase is contradictory to standard CVD trends. However, when compared with the literature on LICVD, this tendency is in good agreement with our previous results[13] and with those of Watanabe et al.[14] obtained with a KrF laser. Watanabe et al. attributed this result to a kinetic influence, favoring rutile over anatase at higher growth rates. However in our case, higher growth rates are obtained at higher substrate temperatures[1] (see Figs. 4c and 4f, the number of pulses required to deposit thin films of same thicknesses). Therefore, it is very likely that a modification in the deposition chemical reaction pathways, depending on substrate temperature, is responsible for these different crystallinities. In fact, Watanabe et al. showed, using either an ArF or a KrF laser, that the irradiation of a condensed TTIP layer or the LICVD from TTIP and O_2, either on the surface or in the gas phase, leads to either anatase or rutile by a complex process which is not clearly understood.[20–22] In our system, thermal CVD, although much slower than LICVD, starts at a substrate temperature higher than 150 °C[1] and may contribute to variations of the nucleation process.

Laser repetition rate is also observed to influence the phase transitions. Figure 7 shows a transition from amorphous to anatase at low fluence, and a transition from anatase to rutile at high fluence with increasing laser repetition rate (from 1 Hz to 5 Hz). This result contradicts those of Watanabe et al.[14] Figure 8 shows that there should be no cumulative heating effect between successive pulses with repetition rates up to the kilohertz range. This fact is also supported by the lack of dependence of the growth rate upon the laser repetition rate and substrate nature, whilst it is highly dependent upon the substrate temperature.[1] Therefore, the laser repetition rate probably also influences crystallite nucleation. Further investigation is necessary in order to understand these nucleation effects.

4. Conclusions

Titanium dioxide thin films are deposited by LICVD without any evidence for non-stoichiometry or bulk carbon contamination for the experimental parameter ranges considered. The deposited film crystallinity varies from amorphous to anatase to rutile, depending on the experimental conditions. The nature of the crystalline state obtained is believed to be due both to various nucleation pathways, and to laser-induced in-situ annealing of the deposited film.

5. Experimental

Deposition System: The experimental set-up of our home-made LICVD reactor was previously reported in detail elsewhere [1]. Briefly, the substrate is placed on a temperature-controlled plate (60–210 °C). A long pulse (250 ns) XeCl excimer laser (308 nm) irradiates the substrate perpendicularly; the image of a mask being projected by a single lens onto the substrate. A pyroelectric detector measures the laser energy and an attenuator regulates the laser fluence on the sample. TTIP is brought into the chamber by an oxygen carrier gas flow, while nitrogen is flushed onto the reactor window to prevent deposition onto it. The total pressure in the chamber is kept at 10 mbar by a closed loop-controlled butterfly valve.

Thin Film Characterization: The deposited thicknesses were measured by profilometry (Tencor Alphastep 200 or Dektak). The thin film chemical composition was measured by XPS, (Kratos Axis Ultra) using irradiation from a monochromated Al Kα source at normal incidence. To compensate for any charging effects, an electron shower is applied and, additionally, all spectra are shifted such that the C_{1s} carbon contamination peak is at 285 eV (characteristic of hydrocarbons). To clean off any surface contamination, sputtering is carried out by a Ar^+ beam at 2 keV with a typical ablation rate of 2 nm min^{-1}. The chemical assay is determined from the area under the peaks, and sensitivity factors.

Raman spectroscopy was used to determine the crystallinity of the deposit material. Two set-ups were used: i) a confocal Raman microscope (Labram, Dilor) in backscattered configuration (light source: Kr^+ laser at 530.9 nm, operated at 100 mW with a 2 μm diameter spot on the sample surface); or ii) a confocal Raman microscope (XY Dilor triple spectrometer) in backscattered configuration (light source: Ar^+ laser at 514.5 nm, operated at 40 mW, with a $10 \times 10 \mu m^2$ spot on the sample surface). Raman spectroscopy is a powerful technique for investigating thin TiO_2 film crystallinity [23]. Amorphous materials give rise to no peaks [24], while the spectrum of a mixture of polycrystalline TiO_2 [24] can be analyzed roughly as a superposition of spectra of different single crystals [25]. The anatase form is characterized by a strong band around 144 cm^{-1} and weaker bands around 399 cm^{-1}, 516 cm^{-1}, 639 cm^{-1} [26]. The rutile Raman spectrum exhibits a band around 235 cm^{-1} due to multiphonon scattering, and two bands at 447 cm^{-1} and 612 cm^{-1} [27].

TEM images were taken of films deposited on silicon. The deposits were first glued with resin and then mechanical polishing of the Si substrate was carried out on the reverse. The resin was then dissolved and the remaining Si substrate was selectively etched in HF-based solutions. The area of the film from which the substrate was completely removed was then analyzed.

Laser-Induced Temperature Rise Calculation: The temperature rise due to laser irradiation was estimated by a numerical simulation. All details of the algorithm used are given in the literature [28]. A spatially uniform laser pulse irradiating a film on a substrate perpendicularly has been modeled. The simulation is based on a simple energy conservation model for small volume element and a small time period. The program considers the temperature change due to the incoming heat (due to light absorption in the material) and outgoing heat (due to heat conduction in the material). This calculation takes into account, the true temporal profile of our laser beam, variation of the optical and thermal properties of the materials (film and substrate) with temperature, and light interference phenomena within the film. The calculation neglects heat generated or lost by chemical reactions, variation of the material properties due to phase changes, and cooling of the substrate by convection or radiation (second order importance parameters).

Even if the program used gives a good temperature estimation [29], the absolute values resulting from the simulations are subject to some uncertainty due to the choice of material property coefficients. However, the trends that are used for the interpretation of the data are not affected.

The thermal and optical parameters (thermal diffusivity, D; thermal capacity, c_p; density, ρ; absorption coefficient, α at 308 nm; and index of refraction, n, at 308 nm), considered for the different materials, are listed in Table 1.

Received: November 26, 2003
Final version: July 12, 2004

Table 1. Thermal and optical properties of the different materials considered for the simulations (values in brackets are temperatures in K). D values are obtained from literature values of thermal conductivity, κ, using the relation $\kappa = \rho \times c_P \times D$. The optical properties of TiO_2, glass, and silicon were measured by ellipsometry [28].

	TiO_2	glass	Si
D [$cm^2\ s^{-1}$]	0.030(293)–0.008(1227) [30]	0.006(293)–0.011(1227) [8]	0.94(293)–0.14(1227) [31]
c_P [$J\ g^{-1}\ K^{-1}$]	0.71(293)–1.523(1227) [30]	0.67(293)–0.92(1227) [8]	0.70(293)–0.95(1227) [31]
ρ [$g\ cm^{-3}$]	3.8	2.76 [8]	2.33
α [cm^{-1}]	2.5×10^5	1	1.5×10^6
n	3.3	1.54	5

[1] E. Halary-Wagner, T. Bret, P. Hoffmann, *Chem. Vap. Deposition* **2005**, *11*, 21.
[2] J. Haigh, M. R. Aylett, *Prog. Quantum Electron.* **1988**, *12*, 1.
[3] I. P. Herman, *Chem. Rev.* **1989**, *89*, 1323.
[4] T. Tsuchiya, A. Watanabe, H. Niino, A. Yabe, I. Yamaguchi, T. Manabe , T. Kumagai, S. Mizuta, *Appl. Surf. Sci.* **2002**, *186*, 173.
[5] N. Asakuma, T. Fukui, M. Aizawa, M. Toki, H. Imai, H. Hirashima, *J. Sol-Gel Sci.* **2000**, *19*, 333.
[6] Y. Ichikawa, K. Setsune, S. Kawashima, K. Kugimiya, *Jpn. J. Appl. Phys. Part 2* **2001**, *40*, L1054.
[7] T. Szorenyi, Z. Kantor, L. D. Laude, *Appl. Surf. Sci.* **1995**, *86*, 219.
[8] T. Szörényi, L. D. Laude, I. Bertoti, Z. Kantor, Z. Geretovszky, *J. Appl. Phys.* **1995**, *78*, 6211.
[9] S.-C. Jung, N. Imaishi, *Korean J. Chem. Eng.* **2001**, *18*, 867.
[10] A. T. Howe, *Photonics Spectra* **1999**, *33*, 126.
[11] T. Sumita, T. Yamaki, S. Yamamoto, A. Miyashita, *Appl. Surf. Sci.* **2002**, *200*, 21.
[12] M. Kadoshima, M. Hiratani, Y. Shimamoto, K. Torii, H. Miki, S. Kimura, T. Nabatame, *Thin Solid Films* **2003**, *424*, 224.
[13] E. Halary, E. Haro-Poniatowski, G. Benvenuti, P. Hoffmann, *Appl. Surf. Sci.* **2000**, *168*, 61.
[14] A. Watanabe, T. Tsuchiya, Y. Imai, *Thin Solid Films* **2002**, *406*, 132.
[15] S. Yamabi, H. Imai, *Chem. Mater.* **2003**, *14*, 609.
[16] E. Halary-Wagner, P. Lambelet, G. Benvenuti, P. Hoffmann, *J. Phys. IV* **2001**, *11*, Pr3-825.
[17] F. Zhang, S. Jin, Y. Mao, Z. Zheng, Y. Chen, X. Liu, *Thin Solid Films* **1997**, *310*, 29.
[18] X.-P. Wang, Y. Yu, X.-F. Hu, L. Gao, *Thin Solid Films* **2000**, *371*, 148.
[19] C. Langlade, B. Vannes, T. Sarnet, M. Autric, *Appl. Surf. Sci.* **2002**, *186*,145.
[20] A. Watanabe, Y. Imai, *Thin Solid Films* **1999**, *348*, 63.
[21] A. Watanabe, T. Tsuchiya, Y. Imai, *Jpn. J. Appl. Phys. Part 1* **2000**, *39*, 120.
[22] T. Tsuchiya, A. Watanabe, Y. Imai, H. Niino, I. Yamaguchi, T. Manabe, T. Kumagai, S. Mizuta, *Jpn. J. Appl. Phys. Part 2* **1999**, *38*, L823.
[23] V. V. Yakovlev, G. Scarel, C. R. Aita, S. Moshizuki, *Appl. Phys. Lett.* **2000**, *76*, 1107.
[24] L. D. Arsov, C. Kormann, W. Plieth, *J. Raman Spectrosc.* **1991**, *22*, 573.
[25] W. Ma, L. Zu, M. Zhang, *Appl. Phys. A–Mater. Sci. Process.* **1998**, *66*, 621.
[26] T. Ohsaka, F. Izum, Y. Fujik, *J. Raman Spectrosc.* **1978**, *7*, 321.
[27] J. F. Mammone, S. K. Sharma, *Solid State Commun.* **1980**, *34*, 799.
[28] E. Wagner, *PhD Thesis*, EPFL, Lausanne **2003**.
[29] E. Halary-Wagner, F. Wagner, P. Hoffmann, *J. Electrochem. Soc.* **2004**, *151*, c571.
[30] *CO_2 Lasers Effects and Applications* (Ed: W. W. Duley), Academic Press, New York **1976**.
[31] *Properties of Optical and Laser-related Materials* (Ed: D. N. Nikogosyan), John Wiley & Sons, Chichester, UK **1997**.

